Relative Composition of Titan's Equator via PCA and *k*-means Clustering N. Kutsop[1] (nwk25@cornell.edu), A. G. Hayes[1,2], C. Sotin[3], J. L. Lunine[1], K. Lawrence[4] , S Le Mouélic[3], S. Rodriguez[5], S. P. D. Birch[6], P. M. Corlies[6] and The Cassini VIMS Team [1]Cornell University, Ithaca NY, [2]Cornell CCAPS, Ithaca NY, [3]LPG, Nantes, France, [4]JPL, Pasadena CA [5]AIM, Gif sur Yvette, France, [6]MIT, Cambridge MA

Introduction: The Visual and Infrared Mapping Spectrometer (VIMS) aboard the Cassini satellite made observations of Titan from 2004-2017 [1]. VIMS consisted of two imaging spectrometers with 352 spectroscopic channels between 0.35 and 5.13 μm. Herein, we analyze data from VIMS using principal component analysis and *k*-means clustering to interrogate the compositional variability of Titan's entire equatorial region, with a focus on Selk Crater (the Dragonfly landing site) [2].

Data: Absorption and scattering by gas and haze alters the spectra of Titan's surface as observed by VIMS. Also because of methane absorption and scattering by haze, only ~48 channels spread throughout the available 352 channels are able to observe the surface. This produces a partial spectrum which is difficult to compare to laboratory spectra. To circumvent the challenges described above we 1) use an empirical model we developed to reduce the effects of scattering and viewing geometry and 2) use a suite of statistical techniques to deduce the relative compositional abundances. These techniques allow us to use nearly the entire VIMS dataset, as opposed to preferentially selecting observations.

To reduce the alteration of the spectra by the atmosphere, we empirically model and remove atmospheric scattering from each observation. We fit a locally weighted scatter smoothing function to a sample of 0.02% of the data, for each flyby. We randomly resample the data through a Monte Carlo simulation with at least 300 runs. This reproduces the smooth manifold created by the haze while ignoring surface features due to their sharp contrast.

We forgo comparing the partial spectra acquired by VIMS to laboratory spectra to determine the absolute composition of a surface feature. Instead, we investigate the relative abundance of principal components across the surface. By reprojecting our spectra into the principal component space we reduce the dimensionality and highlight important spectra which may indicate the abundance of a particular material or feature. When a specific material, such as water ice, is of particular interest we can select the spectral channels where it is most distinctive.

After reprojecting the data into the principal component, we cluster the data using a *k*-means clustering algorithm which uses an iterative process to minimize the distance criterion from an initial set of random cluster centroids. We chose to cluster our data into 16 units, because it is half as many as the channels we used and simplifies analysis.

Results: The 16 clusters determined for the equator through our *k*-means clustering are shown in Figure 1A. Each unit is assigned a unique color in our map. Along with our units we have plotted polygons based on the results of Griffith et al 2019 [3] (CG19 hereafter). These polygons indicate areas CG19 determined to be water ice rich (blue) and water ice poor (green).

We support the claim of an ice corridor in Titan's equator as our clusters show a correlation between the shade of the units identified in CG19 and several of our units. Based on our preliminary correlations, water-ice bearing features are more prevalent than previously proposed. Our units which correlate to CG19's water-ice corridor, seem to preferentially appear on the trailing and leading hemisphere, indicating a potential preference for the formation or retention of water ice.

We see several patterns appear in Figure 1. Certain units appear only in particular sequences, such as those around Menrva, where we see correlation with GC19's identification of water ice or at the boundary where hummocks and plains transition to dunes. This implies that our clusters are identifying areas with a certain relative abundance of material as unique clusters. Furthermore, there is an apparent correlation between geomorphology and the sequence of units. This suggests that the processes responsible for creating and modifying the compositions identified in our clusters are acting across the equatorial region.

We focus our attention on Selk Crater which is the landing site for the Dragonfly mission in the mid-2030s. In Figure 1B we compare Selk to Menrva and Sinlap (two impact craters) and Sotra Patera (a suspected cryovolcanic site). We see that Menrva and Sinlap are similar, showing large areas of units suggestive of water ice enhancements based on comparisons with the areas identified in CG19. **Selk, however, has spectral units that are more similar to Sotra Patera, and shows less in common with Sinlap or Menrva**. In Figure 1B, we see that the units that make up Selk are most commonly seen at the border of dunes and hummock/plains as identified by geomorphologic mapping using Cassini SAR [4]. In Figure 1B, the units which make up Selk never border the units suggestive of water-ice. One possibility is that Selk and the nearby surface may be covered by a layer of organic-rich sediment that obscures water ice signatures, perhaps brought in from the surrounding dune fields.

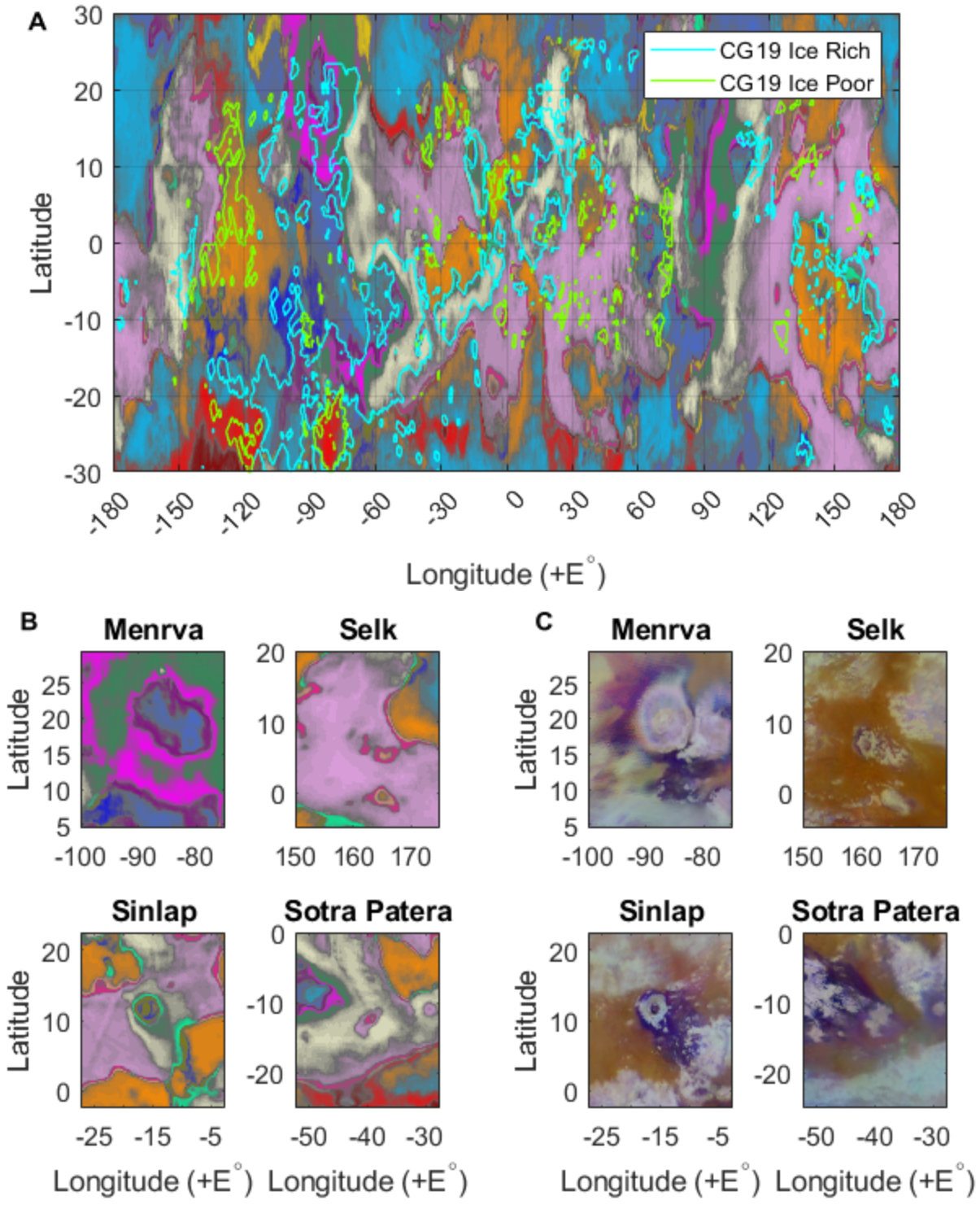

Figure 1: **(*A*)** Equirectangular map of Titan's equatorial region. Colors denote separate units determined through *k*-means clustering. The closer a pixel is to its centroid, the purer the color. The further away a pixel is from its centroid, the grayer the color. **(*B*)** A zoom in of four areas in 1A; Menrva Crater, Selk Crater, Sinlap Crater, and Sotra Patera. **(*C*)** A composite ISS and VIMS map at a higher resolution than our data to provide regional context [5]

References: [1] Brown, R. et al (2004) *SSR, 115: 111–168* [2] Lorenz et al (2019) *APL TechDigest*, *34*, [3] Griffith et al (2019) *Nature Astro 3: 642–648,* [4] Lopes et al (2020) *Nature Astro, 4, 228–233* [5] Le Mouélic et al (2019) *Icarus, 319, 121-132*